# Characterization of semiconductor detectors for $\gamma$-ray and x-ray spectrometry

Author: Helena Boyer López
*Facultat de Física, Universitat de Barcelona, Diagonal 645, 08028 Barcelona, Spain.*

Advisor: José M. Fernández-Varea

Semiconductor detectors are routinely used in $\gamma$-ray and x-ray spectrometry. Their characterization is crucial in order to perform quantitative analysis. Three steps are needed to this end: energy and FWHM calibration and determination of the full-energy peak efficiency. In this TFG we have performed these steps for a HPGe detector. We confirmed the very high linearity, excellent energy resolution and high efficiency of the studied spectrometer.

## I. INTRODUCTION

$\gamma$- and x-ray detectors are used in a wide range of activities, including fundamental research in nuclear and atomic physics as well as applications in materials analysis techniques, radiology, radiological protection, etc. Semiconductor spectrometers made of Si or Ge are the most frequently used due to their excellent energy resolution. The latter are recommended for $\gamma$-ray spectrometry as they have a higher efficiency. In either case, their characterization includes the following steps. 1) Energy vs channel calibration (for peak identification). 2) FWHM vs energy calibration (to quantify energy resolution). 3) Determination of the full-energy (FE) peak (sometimes called photopeak) efficiency (for quantitave analysis).

In this TFG we aim at studying in depth the calibration of a hyperpure Ge (HPGe) spectrometer. We were inspired by an experiment carried out at the "Laboratori de Física Moderna" using a NaI(Tl) detector. There we practiced the first two steps of detector characterization whereas now we went through all the calibration process. No commercial software was used; we rather designed all the required programs so as to fully understand all these aspects.

## II. EXPERIMENTAL SETUP

The experimental part was done at the Servei d'Anàlisi Isotòpica (Facultat de Química) under the supervision of Dr. Joana Tent. We employed a broad-energy HPGe detector, model BE3830 (Canberra, USA) [15]. This planar detector (thickness 30 mm, radius 35 mm) has a good efficiency in the 3 keV–3 MeV interval, with enhanced efficency for low energies due to its thin carbon-epoxy window. The HPGe spectrometer is inside a large shielding made of Pb, Cu and Al that avoids background radiation from reaching the detector.

A series of spectra were measured using point radioactive sources with certified activities. Specifically, the employed sources were $^{22}$Na, $^{60}$Co, $^{133}$Ba, $^{137}$Cs and $^{241}$Am. The sources were placed at 89 mm from the Ge crystal along the symmetry axis to avoid pile-up effects and sum peaks. To ensure they would be placed on the same position we fixed a plastic circle on the detector. A plastic pot fitting in the circle was then put on top, and on its very center the sources were pinned. The measurement time for each source was chosen to be long enough to collect data with good statistics.

The interaction of a $\gamma$ photon with the detector typically produces either a fast photoelectron or a Compton recoil electron. The electron slows down creating many electron-hole pairs. These are then collected by an electric field. The applied electric field also acts on the primary fast electron, changing its energy and thus modifying the position of the peak in the spectrum. This is the so-called field increment effect, but its importance is small. More relevant sources of error in the energy measurement can be live time correction errors, pile-up losses(random summing), true-coincidence summing (two photons arriving at the same time), point-source approximation and losses due to the dead time between detections (after receiving a photon, the detector shuts itself down until the whole signal is collected, to avoid signal overlapping).

## III. PEAK ANALYSIS

Peak analysis requires net spectra, i.e. after removing the natural background caused by cosmic rays as well as $^{40}$K and transuranid radionuclides present in the surrounding. The background was measured for 250 000 s [14], a much longer time than any of our spectra, so it needed to be scaled by a factor $\Delta t/\Delta t_{\mathrm{bg}}$ before subtracting it from the spectra. Figure 1 shows the raw and net spectra of the $^{22}$Na source.

In the net spectrum, some channels with negative counts are found. This is due to the non-negligible fluctuations of the background (and, to a lesser extent, of the radioactive source): the interaction of radiation within the detector is a probabilistic phenomenon.

Despite having subtracted the background (see figure 1), there are counts in channels other than those corresponding to the full-energy deposition peak. Estimating the peak area is therefore not as simple as counting all positive counts as part of the peak. To discriminate in between background and peak points, we needed a reference value: i.e., a counts value over which we considered the channel belonging to the peak, and below which it

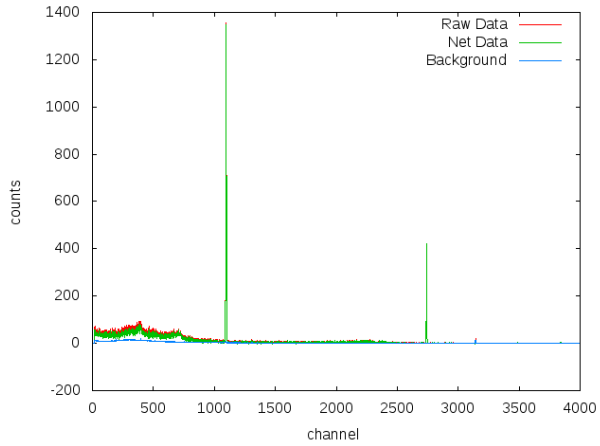


FIG. 1: Spectrum of the $^{22}$Na before and after subtracting the background. The background can be seen in blue.

did not belong to the peak. To this aim, we fitted the measured background to a linear function (via the least-squares method, see section IV). This fit were the values used as a reference to discrimante (non)-peak channels.

The counts that exceed in more than 3 sigma from the fit were considered part of the peak. The beginning of a peak was the channel (belonging to the peak) whose immediate left neighbour did not belong to the peak. Similarly, the end of the peak was the channel (belonging to the peak) whose immediate right neighbour did not belong to the peak.

The shape of x-ray and $\gamma$-ray peaks is Lorentzian due to the finite width of excited atomic and nuclear levels. In turn, energy resolution of semiconductor detectors is Gaussian. The convolution of a Lorentzian and a Gaussian is a Voigt function. However, the width of nuclear levels is much smaller than the resolution of HPGe spectrometers, and therefore the peak shape is well approximated by a Gaussian,

$$G(n) = N\,\frac{1}{\sqrt{2\pi\sigma^2}}\,\exp\left(-\frac{(n-\mu)^2}{2\sigma^2}\right), \qquad (1)$$

where $G$ is the number of counts and $N$ is the area of the peak. Taking the logarithm of $G(n)$ we obtain a second-degree polynomial, which can be fitted using a linear least-squares method. To this end we define

$$I = \sum_i \left[y_i - \left(\alpha + \beta n_i + \gamma n_i^2\right)\right]^2, \qquad (2)$$

where

$$y_i \equiv \ln C_i \qquad (3)$$

$$\alpha \equiv \ln N - \frac{1}{2}\ln(2\pi\sigma^2) - \frac{\mu^2}{2\sigma^2} \qquad (4)$$

$$\beta \equiv -\frac{\mu}{\sigma^2} \qquad (5)$$

$$\gamma \equiv -\frac{1}{2\sigma^2}. \qquad (6)$$

Imposing that $\partial I/\partial\alpha = \partial I/\partial\beta = \partial I/\partial\gamma = 0$ we get a $3\times3$ linear system of equations that is straightforward to solve. As an example of fit, figure 2 displays the 356 keV peak of the $^{133}$Ba source.

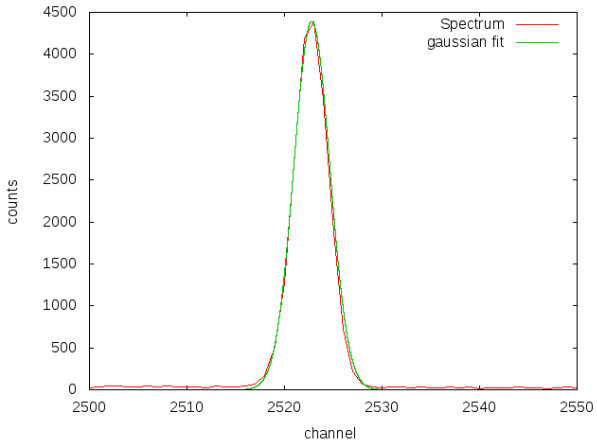


FIG. 2: Spectrum of $^{133}$Co with the Gaussian fit of its second peak shown

The centroid of the peak, $\mu$, follows from the derivative of the Gaussian.

We have computed these values and, comparing the spectra to the theoretical peak energies, we were able to identify the peaks as shown in table I. This will allow, as explained in section IV to relate each channel to an energy.

TABLE I: Identified peaks and their measured channel

| Nuclide | identified channel | $E$ (keV) [13] |
|---|---|---|
| $^{241}$Am | 123.932 | 59.5409 |
| $^{133}$Ba | 762.951 | 356.0129 |
| $^{60}$Co | 2522.97 | 1173.2280 |
| $^{60}$Co | 2866.89 | 1332.5080 |
| $^{137}$Cs | 1420.69 | 661.6570 |
| $^{22}$Na | 2740.78 | 1274.5370 |

The Full Width Half Maximum (FWHM from now on) value of a peak is its width at half the maximum height. Since the peaks have been fitted to Gaussians, the FWHM can be easily computed. Given the maximum height, the channel numbers where the peak will fall to one half are $n = \mu \pm \sqrt{2\sigma^2 \ln\left(y\sqrt{2\pi\sigma^2}\right)}$. The width will be the difference between both values: FWHM $= n_1 - n_2 = 2\sqrt{2\sigma^2 \ln\left(y\sqrt{2\pi\sigma^2}\right)}$. The FWHM will be useful to determine the spectrometer's resolution, as will be seen in section V.

Finally, the peak area also plays an important role in spectrometer characterization, as it is directly related to

the efficiency. We have adopted a very simple method to determine the peak area: we approximated it to a series of rectangles with a 1-channel width. Summing the area of these rectangles, and subtracting the (usually very small) continuum with a linear model, we obtain the net area of the peak.

## IV. ENERGY CALIBRATION

The number of electron-hole pairs is proportional to the energy $E$ of the incident photons. Hence, the height of the collected electrical pulses is also linear in $E$. A multi-channel analyzer (4096 channels) displays the energy spectrum as a histogram as a function of channel number $n$. The relationship between $E$ and $n$ is, to a very good approximation, given by

$$E = a + bn, \tag{7}$$

where $a$ is the offset and $b$ is the gain. These parameters can be found knowing the energies $E_i$ of the $\gamma$-rays emitted by the radioactive sources and the corresponding positions $n_i$ in the spectra.

According to the least-squares method, the best fit of the parameters will be that which minimizes

$$I = \sum_i \left[E_i - (a + bn_i)\right]^2. \tag{8}$$

The partial derivatives of $I$ with respect to $a$ and $b$ must be zero. This gives a simple 2×2 linear system, which has the solution

$$a = \overline{E} - b\overline{n} \qquad \text{and} \qquad b = \frac{\sum_i (n_i - \overline{n})(E_i - \overline{E})}{\sum_i (n_i - \overline{n})^2}. \tag{9}$$

The correlation coefficient of the fit has been computed as well,

$$R^2 = \frac{N\sum_i xy - \sum_i x \sum_i y}{\sqrt{[N\sum_i x^2 - (\sum_i x)^2]\,[N\sum_i y^2 - (\sum_i y)^2]}}. \tag{10}$$

## V. FWHM CALIBRATION

A FWHM-energy relationship needs to be determined in order to set the resolution of the detector. The most commonly used function is

$$\mathrm{FWHM} = \sqrt{c + dE}, \tag{11}$$

where $c$ and $d$ are adjustable parameters. $c$ is the square of the electronic noise that happens during the amplification process. $d$ should be equal to the product of the Fano factor $F$ and the averave energy $W_{\mathrm{eh}}$ required to create an electron-hole pair. Parameters $c$ and $d$ are found using a linear least-squares method that fits $\mathrm{FWHM}^2$ as a function of the energy.

## VI. FULL-ENERGY PEAK EFFICIENCY CALIBRATION

Not all photons that leave the radioactive source will reach the detector. First of all, the detector covers a limited solid angle, which can be determined from the set-up geometry (assuming a point source). The efficiency will be, in first approximation, the geometrical efficiency $\varepsilon_{\mathrm{g}} = \frac{\Omega}{4\pi}$. Secondly, photons may be attenuated by the air or the carbon epoxy window. This attenuation is described by a factor $T(E)$. However, for the energies of the considered $\gamma$-rays we have $T(E) \approx 1$. Only very low-energy photons (below $\sim 50$ keV) are atenuated appreciably by the window ($T(E) < 1$). $T(E)$ and $\varepsilon_{\mathrm{g}}$ determine how many of the emmited photons enter the detector's active volume.

What is the probability that an incoming photon ends up in the FE peak (does not escape, nor does it end up in the Compton edge, nor in a sum-peak)? This is the main question we need to answer in order to know the efficiency of the detector; it is the so-called intrinsic efficiency $\varepsilon$, which depends only upon the detector itself and on the photon energy. From these three components we can deduce that the efficiency can be written approximately as

$$\varepsilon_{\mathrm{FE}}^{\mathrm{th}}(E) = \varepsilon_{\mathrm{g}}(E)\, T(E)\, \varepsilon(E). \tag{12}$$

Electronic timing can have a large effect on the efficiency. After each signal arrives, the detector has some dead time - for sources with a high activity, a large percentage of counts can be lost during the time-out. However, the sources we have used had a rather low activity and our spectrometer's dead time is very short, thus we can neglect this effect. High density sources could have self-absorption distortion of measurements (and therefore decrease of efficiency), but since our sources are not only of a low density but also very small size (not allowing self-absorption), we will consider this correction irrelevant. True coincidence peaks (two photons being detected at the same time) can be very important for multi-$\gamma$ ray sources, as they can alter the true spectrum and decrease the efficiency. For single-$\gamma$-ray peaks like ours, however, this effect can be neglected.

Considering a divergent incoming photon flux, $\varepsilon$ will depend upon the radius with which we illuminate the detector (thickness $L = 30$ mm and radius $R = 35$ mm), the source-spectrometer distance $D = 89$ mm and the spectrometer's active material. The latter is represented by its absorption coefficients, which indicate the interaction probability for each photon. Taking these factors into account, Barros et al. [6] adopt an expression for the intrinsic efficiency that was developed by O'Meara and Campbell [7]. Since the whole detector is illuminated, we have

$$\varepsilon(E) = \frac{\mu_{\mathrm{pe}}}{\mu}\left[1 - \frac{1 - \exp\left[-\mu L\left(\sqrt{1 + (R/D)^2} - 1\right)\right]}{\mu L\left(\sqrt{1 + (R/D)^2} - 1\right)}\, \mathrm{e}^{-\mu L}\right] \tag{13}$$

where $\mu_{\text{pe}}$ and $\mu$ are, respectively, the photoelectric and total attenuation coefficients for Ge [16].

In turn, the experimental FE peak efficiency is the fraction of photons emitted by the detector that end up in the FE peak. We compute $\varepsilon_{\text{FE}}^{\text{exp}}$ as the ratio of count rate $(N_i/\Delta t)$ vs. counts/s emmited (activity $A_i$), weighted with the probability of photons of that particular energy being emmited (yield). The efficiency, which depends on the photon energy, can therefore be expressed as

$$\varepsilon_{\text{FE}}^{\text{exp}}(E_i) = \frac{N_i}{A\, I_i\, \Delta t}, \tag{14}$$

where $N_i$ is the area of the peak, $A$ is the source activity at the time of the experiment, $I_i$ is the yield of the $\gamma$-ray with energy $E_i$ and $\Delta t$ is the acquisition time. It must be noted that the activity of the source needs to be corrected for decay from the certification date (01/03/1997). The spectra were taken on 19/07/2016, thus the activities are $A = A_0\, \mathrm{e}^{-\lambda t}$ where $A_0$ is the certified activity, $t$ is the time elapsed since the source certification[17] and $\lambda$ the decay constant of each radionuclide.

## VII. RESULTS AND DISCUSSION

The energy-channel fit (fig. 3) has given impressing results: $a = 1.630(5)$ keV and $b = 0.4644(5)$ keV/channel, with a correlation coefficient of $R^2 = 0.999\,999\,987$. The close-to-1 value of $R^2$ confirms the almost perfect linearity of the detector. This fit allows peak identification, as the channel number can now be transformed into energy. Every radionuclide has its own set of $\gamma$-ray energies; therefore, being able to identify a peak's energy with high precision, the spectrometer is the perfect tool to identify unknown unstable nuclei.

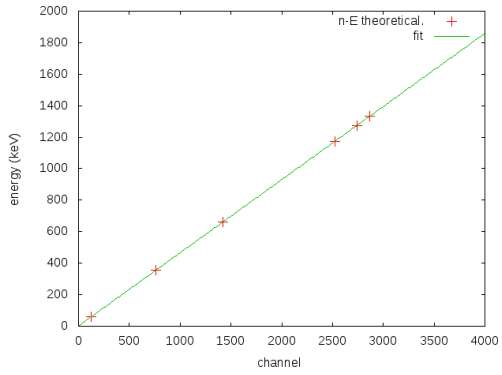


FIG. 3: Energy-channel calibration fit.

We have calculated the energy of the studied peaks using the linear fit. The results showed low discrepancy with the theoretical energies, see table II. In the Servei d'Anàlisi Isotòpica laboratory, a similar fit is being used in order to transform the channels into energy. The two fits have been compared (see table II), and both parameter sets differ in less than their uncertainty. Hence, we can state that the presently obtained results are consistent.

TABLE II: experimental vs. theoretical energy and lab vs. experimental fit values comparison.

| Nuclide | $E_{\text{th}}$ (keV) | $E_{\text{exp}}$ (keV) | discrepancy (%) |
|---|---|---|---|
| $^{241}$Am | 59.541 | 59.184 | 0.600 |
| $^{133}$Ba | 356.013 | 355.942 | 0.020 |
| $^{60}$Co | 1173.228 | 1173.288 | 0.005 |
| $^{60}$Co | 1333.004 | 1332.508 | 0.037 |
| $^{137}$Cs | 661.657 | 661.393 | 0.040 |
| $^{22}$Na | 1274.537 | 1274.439 | 0.008 |
| Parameter | experimental | lab | discrepancy (%) |
| $a$ | 1.630(5) | 1.6301 | 0.029 |
| $b$ | 0.4644(5) | 0.46438 | 0.004 |

The FWHM fit has given excellent results as well, with $R^2 = 0.999\,994$ (see figure 4). The fitted parameters are $c = 0.10(5)$ keV$^2$ and $d = 0.289(2)$ eV. Knowing that $d = FW_{\text{eh}}$, we can compare it to the values found in the literature. With $F$ of Ge being 0.12(1) [8–10] and $W_{\text{eh}} = 2.90$ eV [1, 2, 10], the expected product is $d = 0.29$ eV. The presently obtained value of $d$ agrees, within the quoted uncertainty, with the literature. On the other hand, the electronic noise is $\sqrt{c} = 0.316(2)$ keV, a typical value for HPGe spectrometers. Finally, it is important to mention that the FWHM quantifies the resolution of the detector: the lower it is, the higher the resolution. It varies with the energy (lower resolution for higher energy) and can be computed for all peaks using equation (11).

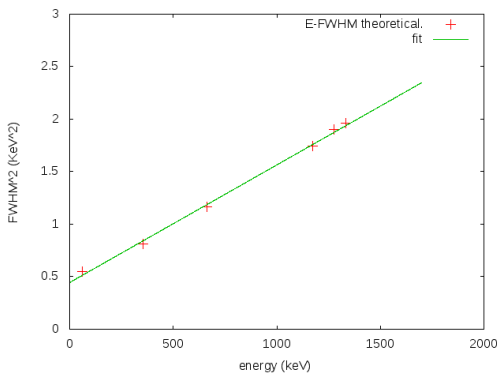


FIG. 4: FWHM-energy fit.

Both the experimental and the theoretical efficiency (fig. 5) show a decrease at higher energies, due to the increasing transparency of the detector. Both show the same behaviour, which is consistent with the one announced by the manufacturer. At low energies, the efficiency is about 85% of the geometrical efficiency, indicating that 85% of the photons that reach the detector

will end up in the FE peak. This is a really good result; few spectrometers provide better ones.

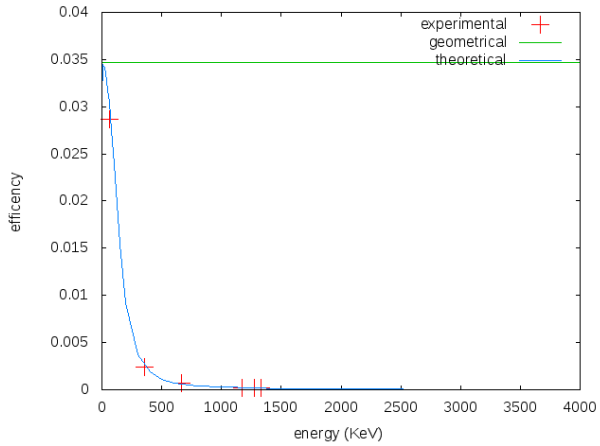


FIG. 5: Efficiency-energy curve

## VIII. CONCLUSIONS

The energy calibration shows that the detector is highly linear, which is a very desired property as it allows easy peak determination. The FWHM calibration provides the detector's resolution, which is critical to value the goodness of future analysis. The narrow peaks seen in the spectra indicate a high resolution, which has been confirmed by the finding of low FWHM. The FE peak efficiency calibration, even though done through a very simple model, has given reasonably good results and will allow a quantitative study of the spectra.

Our results are consistent literature, manufacturer's indications and the calibrations used in lab. Further studies could provide a better efficiency calibration by taking into account factors (such as true coincidence or bulk density) that we have neglected, and using data from more varied sources (different sizes and shapes, as well as other source-detector distances and set-ups).

### Acknowledgments

I want to give my most sincere thanks to my advisor, José María Fernández, for his support and guide through this TFG; to Joana Tent for her help with the experimental part; to Maria Arazo for her advise on programming and to Anna Marit Weisheit for her support and advise concerning the report and presentation.

[1] W. Riegler, *Particle Detectors*, (Summer Student Lectures, CERN, 2010).
[2] K. Vetter, *Recent developments in the Fabrication and Operation of Germanium Detectors*, 3rd. ed. (Livermore National Laboratory, California, 2007).
[3] G.R. Gilmore, *Practical Gamma-Ray Spectroscopy*, 2nd. ed chapters 2, 3, 7 and 9 (John Wiley & sons, 2008).
[4] N. Tsoulfanidis, *Measurement and Detection of Radiation*, 2nd. ed, chapter 7.
[5] G.F. Knoll, *Radiation Detection and Measurement*, 2nd. ed, chapters 4, 11 and 12.
[6] S.F. Barros, N.L. Maidana, J.M. Fernández-Varea and V.R. Vanin, "Full-energy peak efficency of Si drift and Si(Li) detectors for photons with energies above the Si K binding energy". X-Ray Spectrometry **46** 34–43 (2017).
[7] J.M. O'Meara and J.L. Campbell, "Corrections to the conventional approach to Si(Li) detector efficiency". X-Ray Spectrometry **33** 146–157 (2004).
[8] R. Alig, S. Bloom and C. Struck, "Scattering by ionization and phonon emission in semiconductors". Physical Review **B.22.5565** (1980).
[9] S. Croft, D.S. Bond. "A determination of the Fano factor for germanium at 77.4 K from measurements of the energy resolution of a 113 cm3 HPGe gamma-ray spectrometer taken over the energy range from 14 to 6129 keV". (Harwell Laboratory, 1991).
[10] F. Gao, L.W. Campbell, R. Devanathan et al. "Gamma-ray interaction in Ge: A Monte Carlo simulation". Beam Interactions with Materials & Atoms, (2006).
[11] José M. Fernández-Varea, *Radioactividad* (2014).
[12] José M. Fernández-Varea, *Interacción de las radiaciones ionizantes con la materia*. (2014).
[13] Radioactive materials DDEP database; http://www.nucleide.org/DDEP_WG/DDEPdata.html
[14] Calibration and background data from the Servei d'Anàlisi Isotòpica, provided by Joana Tent
[15] Canberra, data and technical data sheet of Broad Energy Germanium detectors
[16] NIST Standard Reference Database, https://www.nist.gov/pml/xcom-photon-cross-sections-database
[17] The number of days between two dates is the output of excel's DIAS function.